



THE UNIVERSITY *of* EDINBURGH

Edinburgh Research Explorer

## **Semi-empirical model for estimating the Heat Release Rate required for flashover in compartments with thermally-thin boundaries and ultra-fast fires**

**Citation for published version:**

Beshir, M, Wang, Y, Centeno, F, Hadden, R, Welch, S & Rush, D 2020, 'Semi-empirical model for estimating the Heat Release Rate required for flashover in compartments with thermally-thin boundaries and ultra-fast fires', *Fire Safety Journal*. <https://doi.org/10.1016/j.firesaf.2020.103124>

**Digital Object Identifier (DOI):**

[10.1016/j.firesaf.2020.103124](https://doi.org/10.1016/j.firesaf.2020.103124)

**Link:**

[Link to publication record in Edinburgh Research Explorer](#)

**Document Version:**

Peer reviewed version

**Published In:**

Fire Safety Journal

**General rights**

Copyright for the publications made accessible via the Edinburgh Research Explorer is retained by the author(s) and / or other copyright owners and it is a condition of accessing these publications that users recognise and abide by the legal requirements associated with these rights.

**Take down policy**

The University of Edinburgh has made every reasonable effort to ensure that Edinburgh Research Explorer content complies with UK legislation. If you believe that the public display of this file breaches copyright please contact [openaccess@ed.ac.uk](mailto:openaccess@ed.ac.uk) providing details, and we will remove access to the work immediately and investigate your claim.



# Semi-empirical model for estimating the Heat Release Rate required for flashover in compartments with thermally-thin boundaries and ultra-fast fires

M. Beshir<sup>a\*</sup>, Y. Wang<sup>a</sup>, F. Centeno<sup>a,b</sup>, R. Hadden<sup>a</sup>, S. Welch<sup>a</sup> and D. Rush<sup>a\*</sup>

<sup>a</sup>School of Engineering, University of Edinburgh, UK,

[M.Beshir@ed.ac.uk](mailto:M.Beshir@ed.ac.uk), [D.Rush@ed.ac.uk](mailto:D.Rush@ed.ac.uk)

<sup>b</sup>School of Engineering, Federal University of Rio Grande do Sul, Porto Alegre, RS, Brazil

\* = Corresponding Authors

## Abstract

More than 1 billion people are living in informal settlements and refugee camps where houses are commonly built from thermally-thin materials (e.g. steel/asbestos sheets). In fire safety literature there is insufficient attention describing the required conditions for flashover (e.g. Heat Release Rate needed for flashover,  $\dot{Q}_{FO}$ ) in such compartments. In this work,  $\dot{Q}_{FO}$  and heat fluxes to the surroundings for compartments with thermally-thin boundaries were investigated using eight compartment fire tests built with 0.5 mm steel sheets and four fuel loads. Numerical simulations were conducted to validate FDS for this application, using the heat release rate inside and outside the compartment, the gas layer temperature and the heat fluxes to the surroundings. The validated model was employed to conduct demonstrative sensitivity and parametric studies to understand the heat balance for thermally-thin under-ventilated compartments. It was found that the heat transfer on/from the walls of the compartment is dominated by radiation, in contrast to the compartments with thermally thick boundaries where the wall conduction dominates. The radiative heat transfer coefficient  $h_{rad}$  was then resolved numerically and correlated against the gas layer temperature, wall temperatures and the  $\dot{Q}_{FO}$  to create a semi empirical correlation for estimating the  $\dot{Q}_{FO}$ .

**Keywords:** compartment fires; heat transfer; CFD; modelling; flash-over, thermally thin

## 1 Introduction

Over 95% of the 180,000 global annual fire deaths occurred [1] in low- and middle- income countries (LMICs) with a considerable portion of these fires occurred within informal settlements (ISs). ISs are at high risk of fires that cause trauma, injury or death. ISs' numbers and sizes globally have increased dramatically in recent years. Affordable and accessible urban housing has not kept pace with rising population growth and as a result, people have been forced to live in low quality informal settlement dwellings (ISDs). The absolute number of IS residents has grown by 213 million since 1990 and this number is still increasing due to rapid urbanization.

To be able to understand the fire risk in these settlements and ultimately to increase their resilience to fires, we need to model the fire spread and to do so, we need to first try to understand how the fire initiates in each dwelling and radiates to the surroundings. Therefore, there is a need to study the fire dynamics and spread within these settlements [2]. In these settlements, dwellings are usually made out of cheap, easily sourced, local materials, which commonly result in combustible (e.g. Timber) or non-combustible thermally-thin construction materials (e.g. Steel sheets) [2]. It is important to note that thermally thin in this paper is defined as materials that have a Biot number of  $10^{-1}$  or less, where the temperature gradient within the solid may be ignored [3].

43 The term “compartment fires” refers to those which are confined within an enclosure that can  
44 be described as a building. The specifications of the enclosure can highly affect the fire  
45 progress/growth within the compartment, i.e. the compartment dimensions, the size of the  
46 openings (ventilations), the lining materials and the wall (boundaries) properties. In the past  
47 few decades, there has been a lot of research on compartment fires and how these specifications  
48 affect different fire stages (growth, fully developed and decay) [3]. The fully-developed fire  
49 stage is also usually referred to as the ‘post-flashover’ stage, where flashover was first defined  
50 and studied quantitatively by Waterman in 1968[4], who defined it as conditional on a heat  
51 flux of 20 kW/m<sup>2</sup> on the floor. The occurrence of flashover in a certain compartment generally  
52 means that the room is well filled with flaming combustion and that the heat fluxes to all the  
53 fuel packages are high enough to cause auto-ignition [5], at this moment the occupant life safety  
54 vanishes.

55 Based on that, the ability to predict the heat release rate needed for flashover ( $\dot{Q}_{FO}$ ) has attracted  
56 extensive attention within the fire safety community, especially in mid 1970s and early 1980s.  
57 Hägglundet and Persson (1976) [6] defined a flashover criteria as 600 °C just below the ceiling  
58 when flames were observed outside of the door. However, more detailed understanding and  
59 definitions of flashover emanated from Babrauskas 1979-1980 [7] and Thomas 1981 [8] who  
60 defined the flashover criteria as an upper gas layer temperature of 600 °C or as radiation on the  
61 floor level of 20 kW/m<sup>2</sup>, and created simple empirical correlations based on the heat balance  
62 for the gas layer within tens of compartment fire tests (with concrete walls) to estimate the  
63 room flashover potential. Thomas [8] included the three heat transfer/exchange mechanisms  
64 from the gas layer to the walls, namely conduction, convection and radiation. This was  
65 followed by the work done in 1981 by McCaffrey et al. (MQH) [9] who analysed more than  
66 100 experimental compartment fires from different tests series using different fuel loads, fuel  
67 types, compartment sizes, ventilation factors and wall materials. The flashover criteria was  
68 taken as 525 °C beneath the ceiling and a heat balance was done on the upper gas layer. A heat  
69 transfer coefficient was developed depending on the duration of the fire, the thermal  
70 characteristics of the compartment’s boundary (namely conductivity, diffusivity, density and  
71 thickness) with mostly inert thermally-thick walls. MQH then suggested an empirical  
72 correlation (Eq.1):

$$73 \quad \dot{Q}_{FO} = 610(h_k A_T A_o H^{\frac{1}{2}})^{1/2} \quad (1)$$

74 where  $h_k$  is the effective heat transfer coefficient,  $A_T$  is the total wall area,  $A_o$  is the opening’s  
75 area and  $H$  is the opening height. One of the main limitations of the MQH is that it doesn’t  
76 consider the growing heat release rate or when the walls of the compartment (boundaries) are  
77 thermally thin (lumped).

78 In 1994, Peatross and Beyler [10] used fifteen natural ventilation and twelve forced ventilation  
79 compartment fire experiments in a steel ship compartment (with 12.7 mm steel boundaries) to  
80 modify the MQH correlation for predicting temperatures in compartments with conductive  
81 boundaries. However, Peatross and Beyler’s correlation was mostly empirical and did not  
82 consider cases with thinner wall thickness (e.g. 0.5 mm steel sheets as those found in ISs), fast  
83 growing fires or different walls’ emissivity which is common to be different in ISs (e.g. clean  
84 steel sheets compared to asbestos sheets).

85 In 2015, Evegren and Wickström [11] developed a simple model to predict the upper layer  
86 temperature-time curve in compartments with lumped boundaries for a given heat release  
87 curve. This model requires inputs like the volume of the compartment, the ventilation factor,  
88 the boundaries’ properties, the fuel/fuel pan details and the HRR-time curve.

89 In the current study the Heat Release Rate needed to reach flashover ( $\dot{Q}_{FO}$ ) is being evaluated  
90 for extremely thermally-thin (Biot number of the order of  $10^{-2}$  or lower) bounded compartments  
91 with boundaries made of steel, aluminium, and asbestos sheets with thickness ranging from  
92 0.5-4 mm with an ultra-fast fire. The study is based on conducting eight small scale  
93 compartment fire tests to validate the Computational Fluid Dynamics (CFD) code Fire  
94 Dynamics Simulator (FDS) [12] using the experimental data from quarter scale ISO 9705 room  
95 [13] fire tests built with carbon steel sheets and using four fuel loads of Polypropylene (PP)  
96 beads in a pan in the middle of the compartment. The validated model is then used to further  
97 understanding of the effect of changing the wall thermal properties and the ventilation factor  
98 value on the  $\dot{Q}_{FO}$ , and the generated data is used to propose a data-based semi-empirical  
99 correlation for estimating the  $\dot{Q}_{FO}$  for these extremely thermally-thin compartments.

## 100 2 Methodology

### 101 2.1 Experimental setup

102 As presented in Fig. 1, a quarter scale ISO-9705 compartment used in the experimental work  
103 was made out of 0.5 mm corrugated steel sheets, with the dimensions of 0.6 m  $\times$  0.9 m  $\times$  0.6  
104 m (L  $\times$  W  $\times$  H) and one opening of 0.2 m  $\times$  0.5 m (W  $\times$  H) on the short wall. The compartment  
105 was placed under a large-scale calorimetry hood with a fan to capture the gas products during  
106 the fire test for the HRR calculations. The HRR measurement was based on the oxygen  
107 consumption calorimetry principle and used measurements of exhaust flow velocity and gas  
108 volume fractions (Oxygen consumption) along with the formulation derived by Janssens[14],  
109 the suggested error for this method is  $\pm 10\%$  for complete combustion and this error increases  
110 with larger amounts of CO or soot produced.

### 111 2.2 Experimental conditions

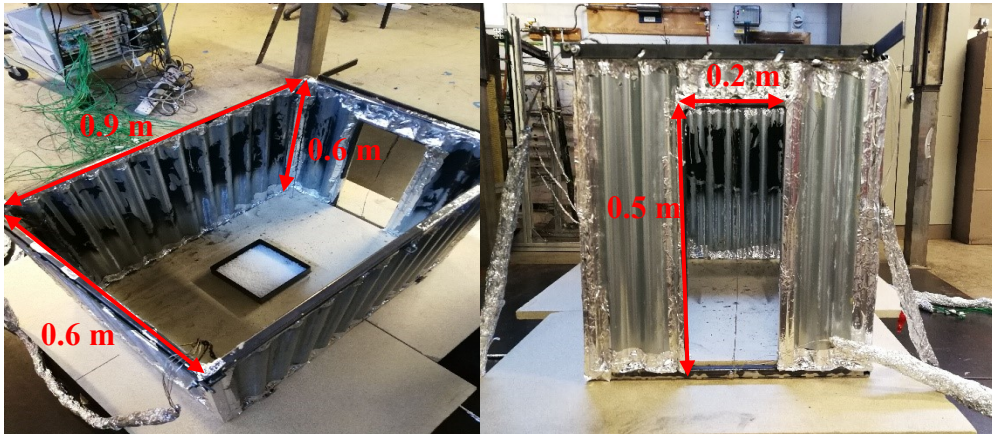
112 In total, eight experiments were conducted, where the ventilation factor, and amount of  
113 accelerant were kept constant (at  $0.0707 \text{ m}^{5/2}$ , and 200 ml of Heptane, respectively). The  
114 ventilation factors ( $Vf$ ) are defined as [15]  $Vf = A_w H^{1/2}$ , where  $A_w$  is the area of the opening  
115 and  $H$  is the height of the opening.

116 Four different fuel loads used to capture the load needed to reach flashover in this compartment  
117 (80, 40, 32, 24 MJ/m<sup>2</sup>, respectively) were then used in two experiments each. The naming  
118 convention for the experiments is thus 80\_1 for the first experiment using a fuel load of 80  
119 MJ/m<sup>2</sup>, and 80\_2 for the second, and so forth for the remaining fuel loads. The fuel used was  
120 the Polypropylene (PP), adopted in order to mimic the burning of solid fuel loads which mainly  
121 consist of hydrocarbons, the fuel pan was 0.4 m  $\times$  0.4 m and placed in the middle of the  
122 compartment. For more information, reference [16] gives detailed information about the  
123 thermal degradation of the PP.

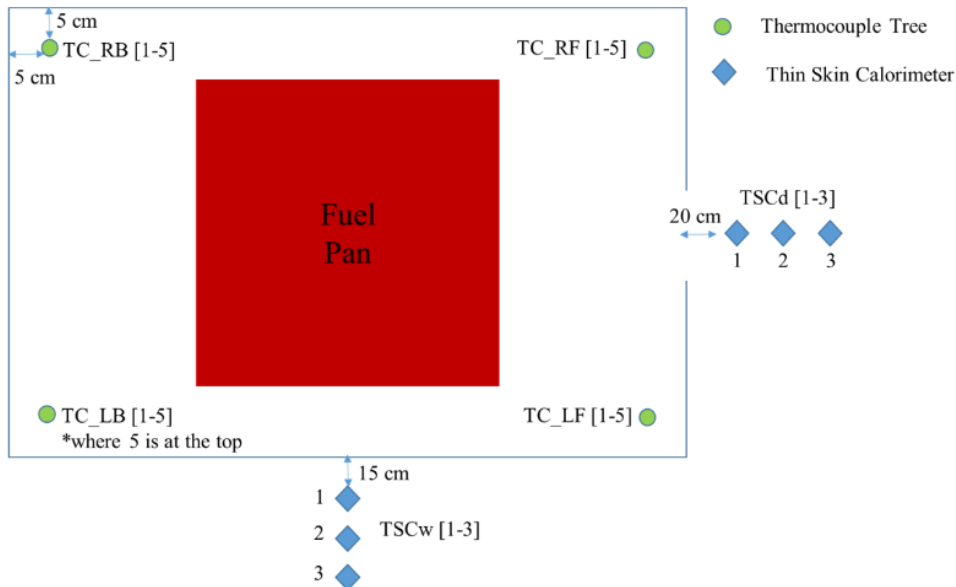
### 124 2.3 Measurement Locations and instrumentation

125 **Thermocouples:** temperatures were recorded at the four corners of the compartment using  
126 four thermocouple tress, each made out of five 1.5 mm Type-K thermocouples (to measure the  
127 gas temperature within the compartment). Each tree was placed at 5 cm from each wall, with  
128 the first thermocouple 10 cm from the floor and the top thermocouple 10 cm from the ceiling  
129 and 10 cm separation distance between the thermocouples in between. The locations are  
130 presented in Fig. 2. **Heat fluxes:** The incident radiative heat fluxes to the surroundings were  
131 calculated using the measured temperatures via the Thin Skin Calorimeters (TSCs) [17] at 20,  
132 40 and 60 cm from the top of the door and 15, 30 and 45 cm from the top of the left wall. **Flow**  
133 **velocity:** The flow velocity was measured at three vertical locations in the middle of the door

134 0.1 m, 0.25 m and 0.4 m from the floor via three bi-directional flow probes. The flow probes  
 135 were designed based on the bi-directional probes proposed by McCaffrey and Heskestad [18]  
 136 and the measured velocities were then corrected by the method proposed by Gupta et al. [19].  
 137



138  
 139 **Fig. 1.** Quarter scale ISO-9705 compartment (open ceiling for demonstration)

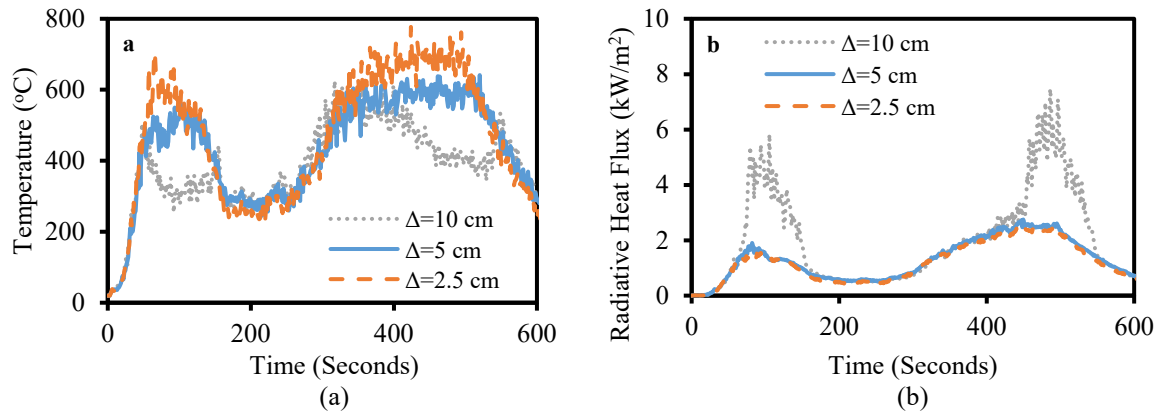


140  
 141 **Fig. 2.** Measurements' locations (Not to scale)

142 **2.4 Numerical setup (Model description and simulations details)**

143 In this study, the Fire Dynamics Simulator (version 6.6.0) [12] was used to model the  
 144 experiments and to do any further parametric studies. The set-up in the model corresponds to  
 145 the experimental set-up reported above, the temperatures were computed by modelling a K-  
 146 type thermocouple of 1.5 mm and the heat fluxes were calculated by using the radiative heat  
 147 flux measuring device in FDS. The fire was represented on a surface with the same location  
 148 and dimensions as the tray used in the experiments and the edges of the tray were modelled  
 149 with the same thickness and material (0.5 cm thickness, 10 cm lip and carbon steel as a  
 150 material), the fire was modelled using the simple pyrolysis model in FDS, where the fire is  
 151 represented by a Heat Release Per Unit Area (HRRPUA) curve corresponding to the  
 152 experimental HRR measured via the Oxygen consumption method. The computational domain  
 153 has been set to X= 1.10 m, Y= 1.5 m and Z= 0.9 m, the cell size used in the simulations was

154  $\Delta = 5$  cm and a cell size sensitivity analysis was conducted as presented in Fig. 3 – three cell  
 155 sizes were tested, namely 10 cm, 5 cm and 2.5 cm. The gas layer temperature was compared  
 156 for each and it was found that the 10 cm cell size case underestimated the temperature in the  
 157 steady state by around 30 % and overestimated the Heat flux at 60 cm from the door by around  
 158 160% compared to the 2.5 cm cell size. However, the 5 cm cell size underestimated the gas  
 159 layer temperature at the steady state by around 10% and overestimated the heat flux at 60 cm  
 160 from the door by around 13% compared to the 2.5 cm cell. Therefore, it was decided to use a  
 161 cell size of 5 cm in this study throughout the whole domain based on a ‘precision  $\times$   
 162 computational time’ evaluation.



163

164 **Fig. 3.** (a) Cell size ( $\Delta = 10, 5,$  and  $2.5$  cm) sensitivity analysis simulations of test 40\_11 for  
 165 gas layer temperature at TC\_LF\_5, and (b) for radiative heat flux at 60 cm from the door

166 For more details regarding the FDS inputs, the PP [20] was used with a Heat of Combustion of  
 167 43.3 MJ/kg, soot yield of 0.058, CO yield of 0.024 and radiative fraction of 37%. The heat  
 168 transfer parameters for carbon steel and the insulation on the floor were: density of 7850 and  
 169 208 kg/m<sup>3</sup>; emissivity of 0.6 and 1.0; specific heat of 0.6 and 0.8 kJ/kg.K; and conductivity of  
 170 48 and 0.1 W/mK, respectively.

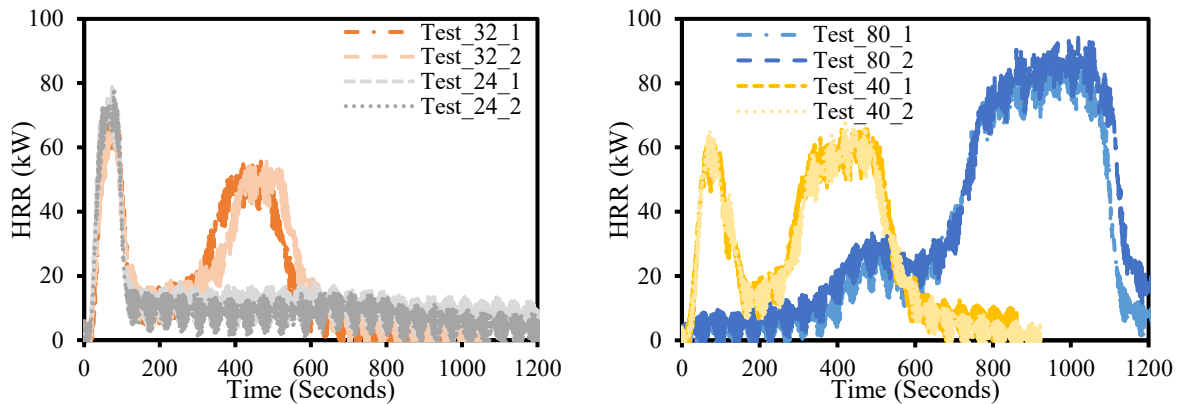
### 171 3 Results and discussion

#### 172 3.1 Repeatability in experimental work

173 As mentioned before, each test was done twice to explore repeatability and as presented in Fig.  
 174 4 the total HRR curves were duplicated with good accuracy for all fuel loads. It was noticed  
 175 that flashover was reached for all fuel loads apart from 24 MJ/m<sup>2</sup>. It was also noticed that there  
 176 are consistently two peaks in the HRR curves, the first peak at around 80 and 500 seconds, for  
 177 the fuel loads 40/32/24 and 80 MJ/m<sup>2</sup>, respectively, as the Heptane accelerant burns away, with  
 178 the other peak occurring when the compartment reached flashover due to the burning of the PP  
 179 at around 300 and 700 seconds, for the 40/32 and 80 MJ/m<sup>2</sup>, respectively. It was also found  
 180 that for lower fuel loads, the HRR spikes related to the Heptane burning were much higher, as  
 181 there is much more space on the tray for the Heptane to burn and for air to be entrained, that  
 182 also could be due to the fewer heat losses with less PP in the tray and eventually a lower endo-  
 183 thermicity. It is also important to note that the Flashover Criteria in this work was taken as that  
 184 of the MQH of 525 °C, where the gas layer temperature for the four fuel loads cases is presented  
 185 in Fig. 5.

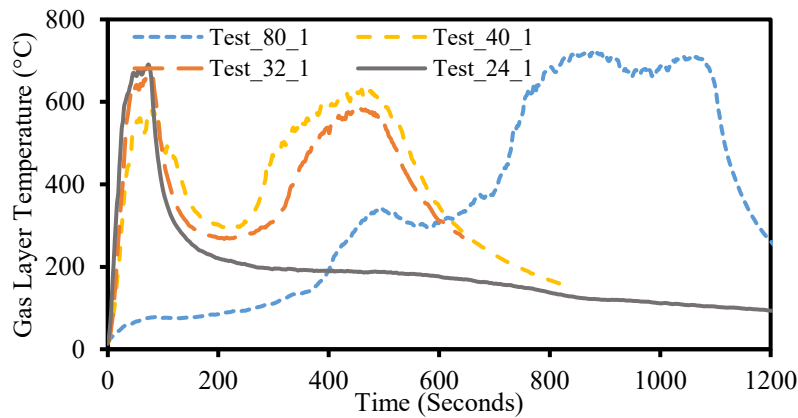
186 It should also be noted that in Tests 32\_1&2 flashover was achieved however flames were  
 187 rarely observed outside of the compartment. This gives a borderline of fuel load needed to  
 188 reach flashover, defined as the fuel where the flashover criteria is reached (525 °C at the steady  
 189 burning of the PP) and most of the burning is happening inside of the compartment. It is

190 assumed that if any lower fuel load was used in this compartment then flashover would not  
191 occur.



192  
193  
194

**Fig. 4.** HRR-time curves evaluation in all tests



195  
196  
197

**Fig. 5.** Gas layer temperatures for all tests at the top of the left front thermocouple tree (TC\_L\_F\_5)

### 198 3.2 Validation

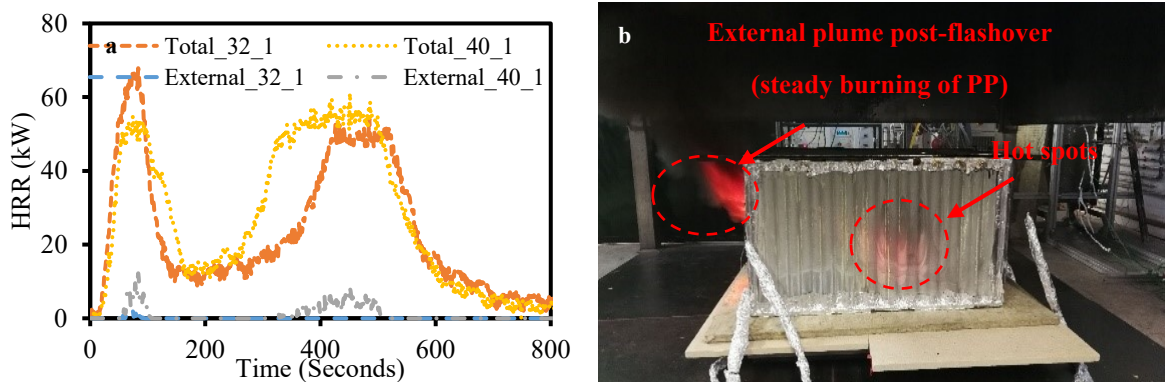
199 To validate the FDS model using these experiments, the HRR-time curves found in Tests  
200 [80\_1, 40\_1, 32\_1 and 24\_1] were used as a ramped input for the FDS (HRRPUA) to model  
201 one test of each fuel load. The measurements of gas layer temperatures in the four corners using  
202 the top thermocouple in each tree were then compared to the corresponding location in the FDS  
203 model, the radiative heat fluxes were calculated using the TSCs and compared to the results  
204 calculated by the ‘Radiative Heat Flux Gas’ device in FDS.

205 One of the main challenges for FDS is modelling under-ventilated compartment fires due to  
206 the complexity when it comes to the combustion (due to the large uncertainties in the  
207 combustion chemistry) and turbulence modelling needed to mimic the real situation.  
208 **Combustion modelling:** FDS’s default combustion model is based on the mixing-limited,  
209 infinitely fast reaction of lumped species and a simple extinction model which is developed  
210 based on one criteria ‘The critical flame temperature value’. In cells with temperature below  
211 this critical value combustion does not occur, as the energy release will not raise the  
212 temperature above the critical value needed for combustion. Therefore, it is important when  
213 using the simple pyrolysis model for combustion in FDS to make sure that the burning is  
214 occurring at the correct locations compared to the experiments. **Turbulence modelling:** FDS

215 is solving turbulence based on the Large Eddy Simulation (LES) technique with the turbulent  
216 viscosity model, Deardorf's[21], as a default.

217 In this work, the HRR peak in test 32\_1 (the borderline case) is assumed to correspond to the  
218 maximum burning that could occur in this compartment; therefore the first validation case was  
219 test 32\_1. This case was used to investigate the ability of FDS to compute all the burning inside  
220 the compartment, before moving to more complex conditions (burning occurring inside and  
221 outside of the compartment), as for tests 40\_1 and 80\_1. In order to compute how much heat  
222 was released at the opening compared to inside of the compartment, in FDS, a device (volume  
223 based) was set outside of the compartment to capture any burning occurring externally.

224 As it is shown in Fig. 6(a) the model presents almost no burning happening outside of the  
225 compartment for test\_32\_1, meaning that FDS managed to compute all the combustion needed  
226 inside of the compartment as observed in the experiments. It is also good to note that when the  
227 Heptane was burning at the beginning of the experiment only around 5 kW were captured by  
228 FDS outside of the compartment. By subtracting this from the total HRR (inside + outside) at  
229 the same time, it could be concluded that the maximum heat release that this compartment  
230 under this configuration can handle inside is around 55-60 kW. To challenge the ability of FDS  
231 to model a longer Post-Flashover fire, the more complex scenario of test 40\_1 with 40 MJ/m<sup>2</sup>  
232 fuel load was simulated. Test 40\_1 had a sustained external plume post-flashover as shown in  
233 Fig. 6 (b). Fig. 6 (a) presents the HRR-time curves for both total and outside the compartment  
234 when modelling test 40\_1 via FDS. It is observed that FDS successfully reproduced the  
235 maximum HRR (burning) inside the compartment for Heptane and PP steady burning, where  
236 the peak HRR inside the compartment was around 55-60 kW. One could then infer that FDS  
237 computed the external plume with an HRR close to that found in the experiments.



238

239 **Fig. 6.** (a) total and external HRR-time curves for Test 32\_1 and Test 40\_1 (FDS)

240

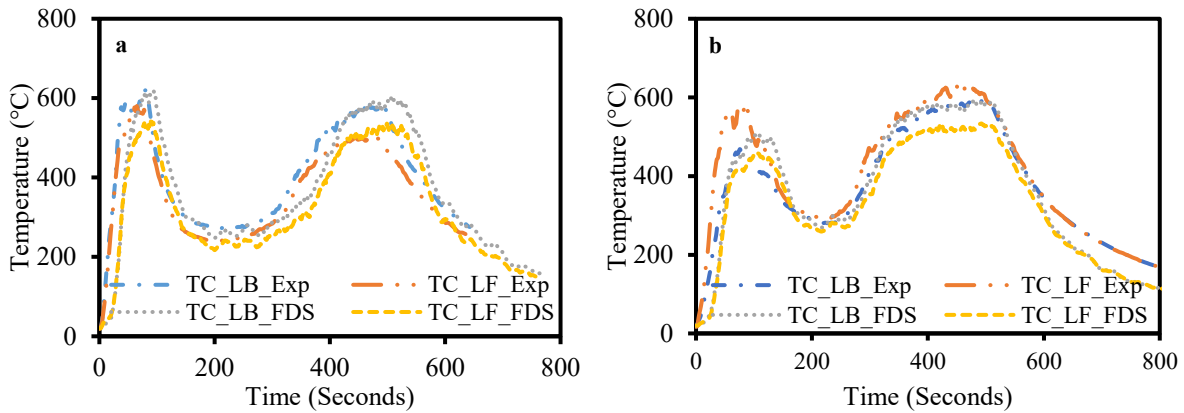
(b) External Plume and heated walls (Test 40\_1)

241 It is also important to investigate the ability of the FDS to compute the combustion in the  
242 correct locations inside the compartment. As presented in Fig. 7 for both tests 32\_1 (a) and  
243 40\_1 (b), FDS managed to capture the same temperature- time curve for the gas layer with  
244 overestimation of around +10% and underestimation of around -15 % compared to the  
245 experiments for tests 32\_1 and 40\_1 respectively, which could give an indication for the  
246 accuracy of the combustion modelling within the compartment (distribution of combustion  
247 inside the compartment). For the sake of completeness, Fig. 8 presents a comparison between  
248 the experimental and numerical results for the thermocouples 1 to 4 of the left front  
249 thermocouple tree for test 40\_1. It was found that the same underestimation occurred along the  
250 height of the thermocouple tree with around -15%, while the very bottom thermocouple's  
251 temperature was overestimated by around +40%.

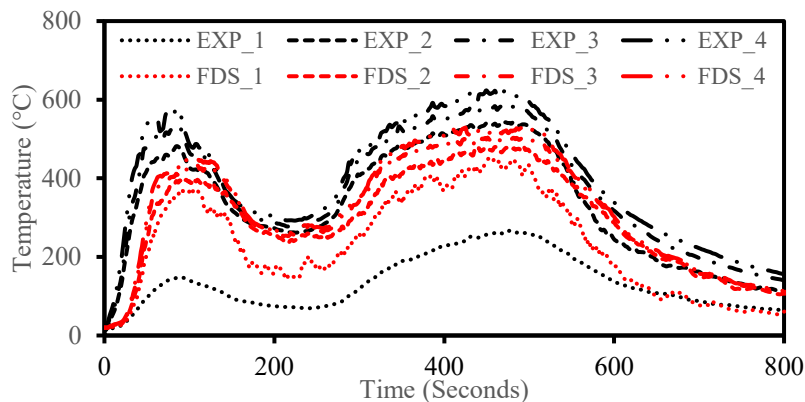


252 To capture the velocities at the door in FDS the total velocity was computed at the same three  
 253 locations as the flow bi-directional probes in the experiments. As presented in Fig. 9 FDS  
 254 captured well the flow through the door at both 0.4 and 0.25 m (also at 0.1 m but not presented  
 255 here) which means that the expected location of the neutral plane for both cases is almost the  
 256 same.

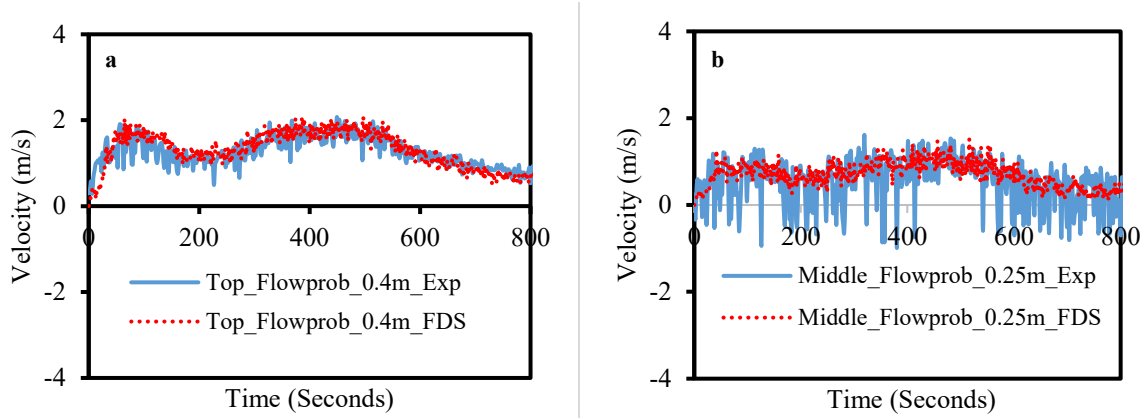
257 As presented in Fig. 10, FDS captured the radiative heat flux trends and values at 60 cm from  
 258 the door and 45 cm from the wall. FDS also computed quantitatively well the radiative heat  
 259 fluxes at 15 cm and 30 cm from the wall, not presented here. However, the TSCs located at 20  
 260 cm and 40 cm from the door were excluded from the analysis due the flame impingement on  
 261 both, which is beyond the current calibration limits for these TSCs. It is also good to note that  
 262 the radiative heat flux from the walls was almost the same value as from the door, which shows  
 263 the effect of the hot thermally-thin walls in radiating to the surroundings (and probably re-  
 264 radiating to the inside of the compartment). All in all, FDS replicated (to a good extent) the  
 265 main measurements, namely heat release rate locations, gas layer temperatures, the radiative  
 266 heat fluxes to the surroundings, and the flow field through the door. Test 80\_1 was also used  
 267 to validate FDS and ended up with very close agreement.



268  
 269 **Fig. 7.** (a) Comparison between the experimental and numerical gas layer temperature-time  
 270 curves Test 32\_1 and (b) Comparison between the experimental and numerical gas layer  
 271 temperature-time curves for Test 40\_1 (Top thermocouples [TC\_5] at two corners)



272  
 273 **Fig. 8.** Comparison between the experimental and numerical results for the thermocouples  
 274 1→4 of the left front thermocouple tree for Test 40\_1

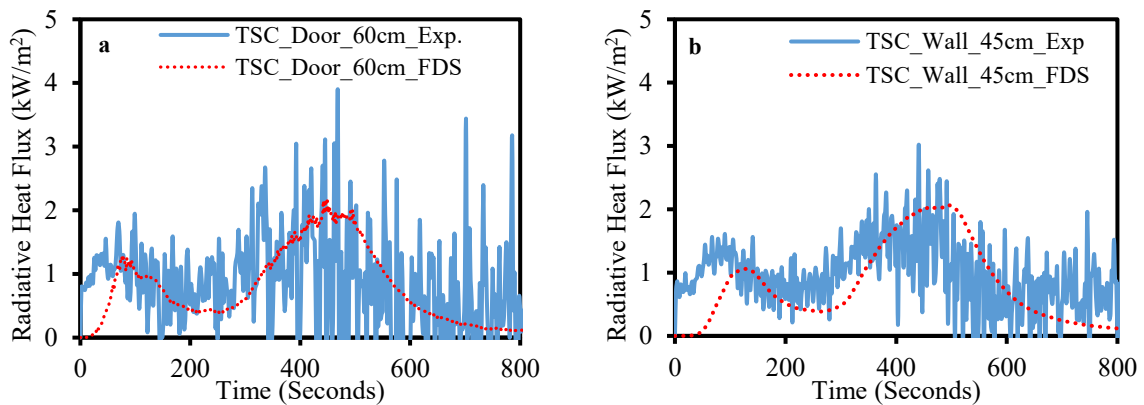


275

276

277

**Fig. 9.** Comparison between the experimental and numerical velocity-time curves at (a) the top and (b) the middle flow probes locations



278

279

280

**Fig. 10.** Comparison between the experimental and numerical Heat Flux-time curves at 60 cm and 45 cm from the (a) the door and (b) the side wall

#### 281 **4 Boundary material and ventilation factor parametric study**

282 To understand the effects of changing the wall properties and ventilation on the  $\dot{Q}_{FO}$ , a  
 283 parametric study was conducted using six different thermally-thin materials (Table 1) and four  
 284 different ventilation factors (Table 2). Under-ventilated compartment fires are considered as  
 285 one of the main challenges to FDS, therefore as our model has been validated with a certain  
 286 ventilation factor, this parametric study will only focus on this and larger opening sizes.

287 ISDs are usually packed with very flammable materials [22] within a very limited space,  
 288 ventilation is always available for the early stages of the fire with the presence of accelerants  
 289 (e.g. methane cylinders for cooking) [23], and therefore, it is assumed to be an ultra-fast  
 290 growing fire. To simulate such conditions, the PP tray (Ramped HRRPUA curve) was replaced  
 291 by a constant HRRPUA burner in FDS, with the same simple pyrolysis model inputs, so it is  
 292 easier to control the HRR within the compartment and also to be able to define the exact  $\dot{Q}_{FO}$   
 293 in each case, where the Flashover criteria was set to be 525 °C at the four corners of the gas  
 294 layer. To define the  $\dot{Q}_{FO}$ , in each case the burner intensity was increased/decreased by 2.5 kW  
 295 till the flashover criteria was reached. Based on the previous experimental analysis the gas  
 296 layer reached 525 °C when the HRR inside of the compartment was around 45 kW, therefore  
 297 45 kW was assumed to be the first guess for this ventilation case. As presented in Table 2, the  
 298  $\dot{Q}_{FO}$  was increased with the ventilation factor and it was generally increased with the  
 299 boundaries' emissivity too.

300 The model developed by Evegren and Wickström [11] captured the temperature-time curve for  
 301 the gas layer in the experiments very well, which means that the model is validated also for  
 302 small scale compartment fires with solid fuels. However, as presented in Table 2 for fast  
 303 growing fires (using a burner) the model did not manage (in most cases) to capture the correct  
 304  $\dot{Q}_{FO}$  with under-predictions between 7 to 24%. Additionally, to use this model a software is  
 305 needed to do the calculations (e.g. Excel) even with no computational time, this model is not  
 306 as simple as an empirical correlation for  $\dot{Q}_{FO}$  (e.g. Eq.1). Therefore, it was deemed important  
 307 to examine a heat transfer model/analysis using the results from this study to create a simple  
 308 empirical correlation to estimate the  $\dot{Q}_{FO}$  for compartments with thermally thin boundaries.

309 **Table 1.** Parametric study materials properties

<b>Material</b>	<b>Thickness <math>\delta</math> (mm)</b>	<b>Emissivity <math>\epsilon</math></b>	<b>Conductivity <math>k</math> (W/mK)</b>	<b>Specific Heat <math>C_p</math> (kJ/kg.K)</b>	<b>Density <math>\rho</math> (kg/m<sup>3</sup>)</b>
<b>Carbon steel</b>	0.5	0.6	48	0.6	7850
<b>Stainless-Steel 304</b> [24]	0.5	0.54	14	0.5	8030
<b>Stainless-Steel clean</b> [24]	0.5	0.26	14	0.5	8030
<b>Stainless Steel lightly polished</b> [24]	0.5	0.19	14	0.5	8030
<b>Aluminium anodized</b> [24]	0.5	0.76	186	1.042	2770
<b>Asbestos</b> [25]	4	0.94	0.58	0.873	1920

310

311 **Table 2.** Parametric study results when varying the materials listed in Table 1 and the  
 312 ventilation factor of the single opening

<b>Ventilation Factor (m<sup>5/2</sup>)</b>	<b><math>\dot{Q}_{FO}</math> (kW)</b>					
	Carbon Steel FDS/[11]	Stainless-Steel 304 FDS/[11]	Stainless-Steel Clean FDS/[11]	Stainless-Steel lightly polished FDS/[11]	Aluminium anodized FDS/[11]	Asbestos FDS/[11]
<b>0.0707</b>	45/45	45/45	40/37.5	40/35	50/45	47.5/45
<b>0.1060</b>	52.5/52.5	55/52.5	50/45	45/42.5	57.5/50	55/52.5
<b>0.1414</b>	72.5/60	70/60	57.5/50	55/47.5	65/57.5	65/57.5
<b>0.1767</b>	85/65	80/65	67.5/55	60/52.5	72.5/62.5	70/62.5

313

## 314 5 Heat Transfer model explanation

315 This section presents, a heat transfer analysis for the compartment, conducted to create a semi-  
 316 empirical correlation to estimate the  $\dot{Q}_{FO}$  with two simple step calculations.

317 As discussed earlier, the rate of heat release at the onset of flashover can be obtained from  
 318 several correlations from the literature (e.g.[5];[8]), while the most popular correlation is the

319 MQH empirical correlation ([9]). Computing the  $\dot{Q}_{FO}$  for the current small-scale compartment  
 320 numerical and experimental work resulted in  $\dot{Q}_{FO}$  values much higher than those observed in  
 321 the experiment/simulations, being  $10^3$  times higher or more. This behaviour can be attributed  
 322 to  $h_k$ , since the materials considered in the present work are in general highly conductive,  
 323 leading to very high values for  $h_k$ , and therefore  $\dot{Q}_{FO}$  from Eq.1. Based on these findings, an  
 324 alternative methodology must be developed to describe the relationship between  $\dot{Q}_{FO}$  and the  
 325 heat transfer through the walls and ceiling of the compartment. The heat fluxes (both  
 326 convective and radiative) on the internal walls and ceiling will eventually be transferred to the  
 327 external ambient environment through conduction, convection and radiation. Taking into  
 328 account the thermal resistances by conduction through the boundary, convection on/from the  
 329 internal/external surface of the boundary, and radiation on/from the internal/external surface  
 330 of the boundary, an overall heat transfer coefficient ( $U$ ) can be defined as:

$$331 \quad U = (R_{cond} + R_{EQ\ In} + R_{EQ\ Out})^{-1} = \left(\frac{\delta}{k} + \left(\frac{1}{h_{conv}+h_{rad}}\right)_{In} + \left(\frac{1}{h_{conv}+h_{rad}}\right)_{Out}\right)^{-1} \quad (2)$$

332 where  $In$  refers to the internal surface,  $Out$  refers to the external surface,  $h_{conv}$  is the convective  
 333 heat transfer coefficient, computed using correlations for free convection [24], and  $h_{rad}$  is the  
 334 radiative heat transfer coefficient, computed as:  $h_{rad} = \epsilon\sigma(T_B^2 + T_S^2)(T_B + T_S)$ , where  $\epsilon$  is the  
 335 surface emissivity,  $\sigma$  is the Stefan-Boltzmann constant ( $5.67 \times 10^{-8}$  W/(m<sup>2</sup>.K<sup>4</sup>),  $T_B$  is the  
 336 temperature of the boundary/wall and  $T_S$  is the temperature of the surroundings. In this study,  
 337 it was considered that  $T_B$  is uniform on the walls (taken as an averaged value for nine points on  
 338 the wall, three points on the left corner, three on the right corner and three on the middle. The  
 339 points were equally distributed vertically bottom, middle and top of each section) and on the  
 340 ceiling (this is a reasonable consideration, since the walls have low Biot number and the  
 341 thermal gradient could be ignored), and  $T_S$  was considered as the hot gas temperature when  
 342 analysing the internal heat transfer resistance ( $R_{EQ\ In}$ ) and as the ambient temperature when  
 343 analysing the external heat transfer resistance ( $R_{EQ\ Out}$ ). Eq.2 must be computed separately for  
 344 walls and ceiling, obtaining  $U_{Wall}$  and  $U_C$ , respectively. Then, the overall heat transfer  
 345 coefficient taking into account all boundaries is obtained from Eq.3, where,  $A_{Wall}$  is the wall  
 346 area,  $A_C$  is the ceiling area and  $A_T$  is the total wall and ceiling area

$$347 \quad U_{Wall+C} = \frac{A_{Wall}}{A_T} U_{Wall} + \frac{A_C}{A_T} U_C \quad (3)$$

348 Fig.11 presents the rate of heat release at the onset of flashover ( $\dot{Q}_{FO}$ ) as a function of the  
 349 overall heat transfer coefficient ( $U_{Wall+C}$ ) for the boundary materials (asbestos board, stainless  
 350 steel, aluminium, carbon steel) and for the different ventilation conditions considered in this  
 351 study. This figure clearly shows that  $\dot{Q}_{FO}$  can be related to  $U_{Wall+C}$ ,  $A_T$  and  $V_F$ . As a first attempt  
 352 for improving the predictions of  $\dot{Q}_{FO}$ ,  $h_k$  was replaced by  $U_{Wall+C}$  in Eq.1, which led to  
 353 significantly better predictions, but still 10 times higher than the experimental values.

354 This first approach suggests that the consideration of a heat transfer coefficient that takes into  
 355 account conduction, convection and radiation would be better for describing the relationship  
 356 between  $\dot{Q}_{FO}$  and the heat transfer mechanisms for thermally thin bounded compartments. This  
 357 is despite the fact that the correlation in Eq.1 is apparently not adequate to this scenario (ultra-  
 358 fast fires and thermally thin boundaries). Since the thermal resistance by conduction ( $R_{cond}$ ) is  
 359 very small, its influence on  $U$  is negligible.

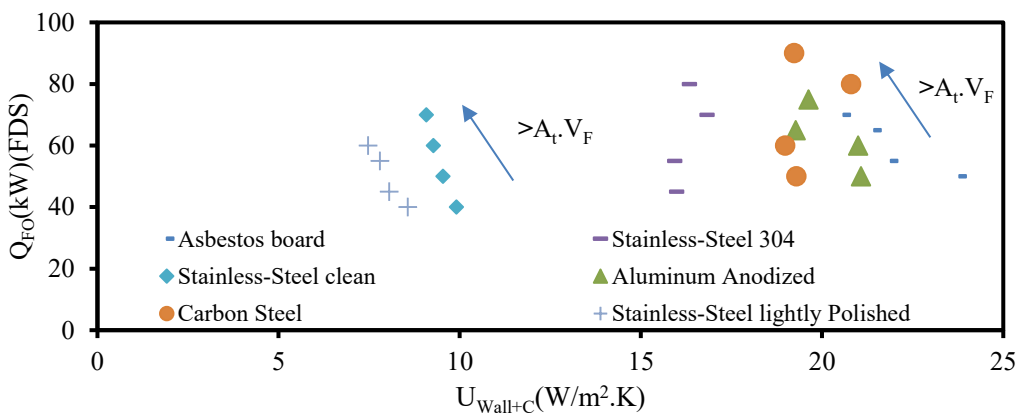
360 For all fires scenarios considered, the convective heat transfer coefficient ( $h_{conv}$ ) for the walls  
 361 and the ceiling, both internal and external, are in the range 1.0-6.0 W/(m<sup>2</sup>.K), so, despite the  
 362 convective thermal resistance not being negligible, there is not a broad variation on this

363 parameter that would explain the variation of  $\dot{Q}_{FO}$  for the different fire scenarios. The same can  
 364 be stated when comparing the radiative heat transfer coefficient ( $h_{rad}$ ) for the walls and the  
 365 ceiling, both internal and external. Those coefficients varied from 15 to 100 (W/m<sup>2</sup>.K) for the  
 366 fire scenarios considered, but for each fire scenario, they did not present a significant difference  
 367 when comparing the values obtained for the walls and for the ceiling. Fig. 12 shows the rate  
 368 of heat release at the onset of flashover  $\dot{Q}_{FO}$  as a function of the radiative heat transfer  
 369 coefficient of the internal walls ( $h_{rad,walls,IN}$ ), for several boundary materials and ventilation  
 370 conditions. This figure is very similar to Fig.11, so the replacement of  $U_{Wall+C}$  by  $h_{rad}$  (for the  
 371 internal wall) is a good choice, since this parameter is simpler to obtain than  $U_{Wall+C}$ , and the  
 372 behavior of  $\dot{Q}_{FO}$  for both parameters  $U_{Wall+C}$  and  $h_{rad,walls,IN}$  is essentially the same. Finally, a  
 373 new correlation was fit to predict  $\dot{Q}_{FO}$  as an alternative to Eq.1. The linear regression was  
 374 performed using a IBM-SPSS software [26], and the input data were those from Table 1  
 375 (materials properties) Table 2 ( $\dot{Q}_{FO}$  data from FDS).

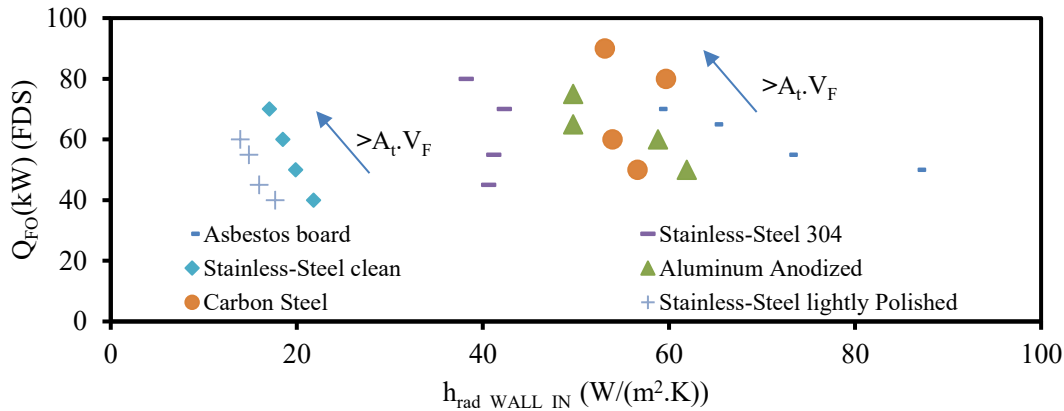
$$376 \quad \theta_{rad} = 10^{7.542} (\epsilon \sigma A_T A_W H_W^{\frac{1}{2}})^{-0.117} \quad (4)$$

$$377 \quad \dot{Q}_{FO} = 10^{19.606} \theta_{rad}^{-2.099} \quad (5)$$

378 where  $\theta_{rad}$  is defined as  $(T_B^2 + T_S^2)(T_B + T_S)$ . Equations 4 and 5 are used together to predict  
 379 the rate of heat release at the onset of flashover ( $\dot{Q}_{FO}$ ) using as inputs only the wall emissivity  
 380 ( $\epsilon$ ), the total area ( $A_T$ ), and the ventilation factor ( $V_f$ ). Fig. 13 shows a comparison of the rate  
 381 of heat release at the onset of flashover ( $\dot{Q}_{FO}$ ) obtained from the new correlation, Eq.5, and  
 382 results from FDS (input data for the regression process). Blue markers denote data conditions  
 383 used to fit Eq.5. It is noted that all blue markers present a maximum of  $\pm 25\%$  agreement,  
 384 demonstrating that the new correlation properly represents the considered fire scenarios. The  
 385 proposed correlation was then tested for eight additional computational fire scenarios,  
 386 considering two different materials (stainless steel,  $\epsilon = 0.68$  and  $\epsilon = 0.33$ ) and four ventilation  
 387 conditions. The red markers on Fig. 13 denote such external validation, using data from these  
 388 eight additional fire scenarios. It is observed that all red markers are within the  $\pm 25\%$   
 389 boundaries with accuracy around  $\pm 15\%$ , so the validity of the proposed correlations for fire  
 390 scenarios other than those used to fit them are adequately shown.

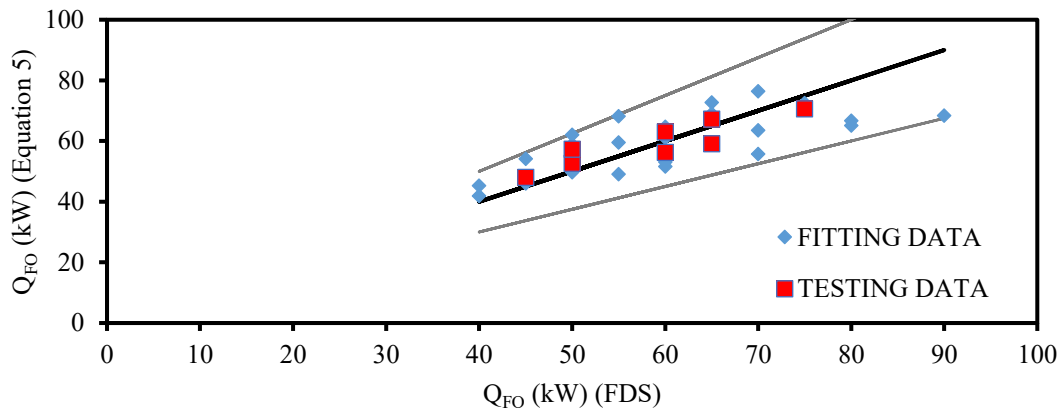


391  
 392 **Fig.11.** Rate of heat release at the onset of flashover ( $\dot{Q}_{FO}$ ) as a function of the overall heat  
 393 transfer coefficient ( $U_{Wall+C}$ ) for several boundary materials and ventilation conditions



394

395 **Fig. 12.** Rate of heat release at the onset of flashover ( $\dot{Q}_{FO}$ ) as a function of the radiative heat  
 396 transfer coefficient ( $h_{rad}$ ) of the internal walls, for several boundary materials and ventilation  
 397 conditions



398

399 **Fig. 13.** Rate of heat release at the onset of flashover ( $\dot{Q}_{FO}$ ): comparison of Eq. (5) outputs  
 400 and results from FDS used as inputs to fit Eq. (5). Blue markers denote data conditions used  
 401 to fit Eq. (5). Red markers denote external computational validation data used to test the new  
 402 correlation

403

## 404 6 Sensitivity analysis

405 To prove the findings in the previous analysis, it was essential to conduct a sensitivity analysis  
 406 for two compartments: one is thermally thin (Carbon steel case) and the other is thermally thick  
 407 with a 13 mm Cement Asbestos wall (with its properties taken from [9] and was used to produce  
 408 the MQH equation). The sensitivity analysis is undertaken for the compartment with the first  
 409 ventilation factor of  $0.0707 \text{ m}^{5/2}$  for both cases. The burner intensity used for the thermally thin  
 410 case was 45 kW and the fire duration was set to 1300 seconds. The compartment with thermally  
 411 thick boundaries was found to reach flashover with 30 kW for the same ventilation factor, so  
 412 the 30 kW burner and 1300 seconds fire was used for the compartment with thermally thick  
 413 boundaries. The sensitivity analysis of the thermal parameters is presented in Table 3 where  
 414 the bold number is the value used in the base case to compare the effect of decreasing  $\downarrow$  or  
 415 increasing  $\uparrow$  the value of each parameter on the gas layer for TC\_LF\_5 and the Radiative Heat  
 416 flux on the front right corner on the floor. Firstly, it was found that the compartment did not  
 417 reach flashover in the thermally-thin case when the emissivity was increased to 0.95 and did  
 418 not reach flashover when the conductivity of 14 W/m.K was used for the thermally-thick case.  
 419 Based on the pervious heat transfer analysis, the main heat transfer mechanism in the

420 compartments with thermally-thin boundaries was radiation, and based on the MQH equation's  
 421 analysis, the conductivity is the main mechanism in the thermally-thick compartments. The  
 422 sensitivity analysis presented in Table 3 validates both assumptions especially for the thermally  
 423 thin case, where it was found that conductivity has almost no effect on the fire dynamics.  
 424 Conductivity was found to be dominating for the thermally thick, as expected, however, the  
 425 sensitivity analysis shows that emissivity could also have some significant effect on the amount  
 426 of radiation from the walls to the fuel packages within the compartment; this needs more  
 427 investigation to be fully evaluated.

428 **Table 3.** Sensitivity analysis for the effect of the conductivity and emissivity on the gas layer  
 429 temperature and heat flux on the floor for thermally thin and thermally thick compartments

Thermally Thin				
	Gas Layer Temperature (LF_5)		Heat Flux on the floor	
<b>Conductivity, k</b> (W/m.K) (0.48↓ -4.8- 48↑)	<b>0.48↓</b>	<b>48↑</b>	<b>0.48↓</b>	<b>48↑</b>
	0.9%	-0.2%	3.1%	-0.48%
<b>Emissivity, ε</b> (0.1↓ -0.6- 0.95↑)	<b>0.1↓</b>	<b>0.95↑</b>	<b>0.1↓</b>	<b>0.95↑</b>
	22.7%	No Flashover	178.4%	No Flashover
Thermally Thick				
	Gas Layer Temperature (LF_5)		Heat Flux on the floor	
<b>Conductivity, k</b> (W/m.K) (0.48↓ -4.8- 48↑)	<b>0.48↓</b>	<b>48↑</b>	<b>0.48↓</b>	<b>48↑</b>
	18.2%	No Flashover	89.8%	No Flashover
<b>Emissivity, ε</b> (0.1↓ -0.6- 0.95↑)	<b>0.1↓</b>	<b>0.95↑</b>	<b>0.1↓</b>	<b>0.95↑</b>
	0.9%	-0.9%	38.7%	-8.6%

430

## 431 7 Conclusions and future work

432 An experimental and numerical study was undertaken to understand the heat transfer  
 433 mechanisms within compartments with thermally-thin boundaries + fast growing fires, and an  
 434 empirical correlation was developed that describes the Heat Release Rate (HRR) needed for  
 435 flashover  $\dot{Q}_{FO}$ . These findings were compared to observations for similar conditions in  
 436 thermally-thick compartments in order to understand the main differences in the heat transfer  
 437 mechanisms.

### 438 The following points were concluded:

- 439 • FDS was validated using eight under ventilated compartment fires with thermally-thin  
 440 boundaries, where the gas layer temperature, flow through the openings, the heat fluxes to  
 441 the surroundings and the HRR inside/outside of the compartment were matching the  
 442 experimental results with around 10-15% variation.
- 443 • An extensive parametric study showed that the wall emissivity was the main heat transfer  
 444 parameter for the  $\dot{Q}_{FO}$  calculations for the walls of the thermally-thin compartments.
- 445 • An empirical correlation was conducted to estimate the  $\dot{Q}_{FO}$  for thermally-thin  
 446 compartments with ultra-fast growing fires (burners) based on the emissivity of the walls,  
 447 the total walls area and the ventilation factor.

- 448 • The empirical correlation was tested numerically and showed very good accuracy, with  
449 less than 15% variation.
- 450 • A sensitivity analysis for the main heat transfer parameters was done on thermally-thin  
451 and thermally-thick compartments, where it was confirmed that the main parameters for  
452 heat transfer for the walls in the former is emissivity and for the latter are conductivity and  
453 emissivity.
- 454 • Some limitations of the model: The  $\dot{Q}_{FO}$  correlation is based on  $0.19 \leq \varepsilon \leq 0.94$ , small scale  
455 compartment with ultra-fast fires and thermally thin boundaries.

456 **For future work:**

457 This work is the first of a series of thermally thin small- and large-scale compartment fires to  
458 further understanding the heat transfer mechanism and the fire dynamics in these compartments  
459 and future work will focus on:

- 460 • The effect of leakage (to better simulate the ISDs into more details)
- 461 • A wider range of ventilation factors.
- 462 • Different fire scenarios (e.g. fast/medium/slow fires).

463 **8 Acknowledgments**

464 This work is supported by IRIS-Fire project of UK (Engineering and Physical Sciences  
465 Research Council Grant no.: EP/P029582/1). Author FRC thanks CNPq/Brazil for research  
466 grant 205477/2018-6.

467 **9 References**

- 468 [1] WHO, “Global Health Estimates 2016: Estimated deaths by cause and region, 2000-  
469 2016, Disease burden and mortality estimates: CAUSE-SPECIFIC MORTALITY,  
470 2000-2016,” 2018.
- 471 [2] Rush, D., G. Bankoff, G. Spinardi, L. Hirst, S. Jordan, J. Twigg, R. Walls and L.  
472 Gibson “Fire Risk Reduction in an Urbanizing World” *GARI9 Contrib. Pap. UNISDR*,  
473 2019.
- 474 [3] D. Drysdale, *An Introduction to Fire Dynamics*. John Wiley and Sons, Chichester,  
475 2011.
- 476 [4] T. E. Waterman, “Room flashover---Criteria and synthesis,” *Fire Technol.*, vol. 4, no.  
477 1, pp. 25–31, Feb. 1968.
- 478 [5] V. Babrauskas, “Estimating room flashover potential,” *Fire Technol.*, vol. 16, no. 2,  
479 pp. 94–103, May 1980.
- 480 [6] B. Hagglund and L. E. Persson, *An experimental study of the radiation from wood*  
481 *flames*. FOA, 1976.
- 482 [7] V. Babrauskas, “Full scale burning behaviour of upholstered chairs,” *Natl. Bur. Stand.*  
483 *NBS Tech. Note No. 1103*, 1979.
- 484 [8] P. H. Thomas, “Testing products and materials for their contribution to flashover in  
485 rooms,” *Fire Mater.*, vol. 5, no. 3, pp. 103–111, 1981.
- 486 [9] B. J. McCaffrey, J. G. Quintiere, and M. F. Harkleroad, “Estimating room  
487 temperatures and the likelihood of flashover using fire test data correlations,” *Fire*  
488 *Technol.*, vol. 17, no. 2, pp. 98–119, May 1981.
- 489 [10] M. Peatross and C. Beyler, “Thermal Environment Prediction In Steel-bounded



- 490 Preflashover Compartment Fires,” *Fire Saf. Sci.*, vol. 4, pp. 205–216, 1994.
- 491 [11] F. Evegren and U. Wickström, “New approach to estimate temperatures in pre-  
492 flashover fires: Lumped heat case,” *Fire Saf. J.*, vol. 72, pp. 77–86, Feb. 2015.
- 493 [12] K. McGrattan, S. Hostikka, R. McDermott, J. Floyd, C. Weinschenk, and K. Overholt,  
494 “Fire Dynamics Simulator Technical Reference Guide. Volume 3: Validation,” vol. 3,  
495 p. 706, 2017.
- 496 [13] “ISO9705: Fire Tests- Full-Scale Room Test for Surface Products First Edition,” 1993.
- 497 [14] M. L. Janssens, “Measuring rate of heat release by oxygen consumption,” *Fire  
498 Technol.*, vol. 27, no. 3, pp. 234–249, Aug. 1991.
- 499 [15] K. Kawagoe, “Fire Behavior in Rooms,” Report 27, Building Research Institute,  
500 Ministry of Construction, Tokyo, Japan, 1958.
- 501 [16] E. Ranzi, M. Dente, T. Faravelli, G. Bozzano, S. Fabini, R. Nava, V. Cozzani, L.  
502 Tognotti, “Kinetic modeling of polyethylene and polypropylene thermal degradation,”  
503 *J. Anal. Appl. Pyrolysis*, vol. 40–41, pp. 305–319, May 1997.
- 504 [17] J. P. Hidalgo, C. Maluk, A. Cowlard, C. Abecassis-Empis, M. Krajcovic, and J. L.  
505 Torero, “A Thin Skin Calorimeter (TSC) for quantifying irradiation during large-scale  
506 fire testing,” *Int. J. Therm. Sci.*, vol. 112, pp. 383–394, Feb. 2017.
- 507 [18] B. J. McCaffrey and G. Heskestad, “A robust bidirectional low-velocity probe for  
508 flame and fire application,” *Combust. Flame*, vol. 26, pp. 125–127, Feb. 1976.
- 509 [19] V. Gupta, C. Maluk, J. L. Torero, and J. P. Hidalgo, “Analysis of convective heat  
510 losses in a full-scale compartment fire experiment,” *Proc. Ninth Int. Semin. Fire  
511 Explos. Hazards*, pp. 490–501, 2019.
- 512 [20] “SFPE handbook of fire protection engineering Published by the National Fire  
513 Protection Association, National Fire Protection Association, Inc., One Batterymatch  
514 Park Quincy, Massachusetts,” no. 5th eddition, 2016.
- 515 [21] J. W. Deardorff, “Stratocumulus-capped mixed layers derived from a three-  
516 dimensional model,” *Boundary-Layer Meteorol*, vol. 18, no. 4, pp. 495–527, 1980.
- 517 [22] Y. Wang, C. Bertrand, M. Beshir, C. Kahanji, R. Walls, D. Rush “Developing an  
518 experimental database of burning characteristics of combustible informal settlement  
519 dwelling materials,” *Under review*.
- 520 [23] R. Walls, G. Olivier, and R. Eksteen, “Informal settlement fires in South Africa: Fire  
521 engineering overview and full-scale tests on ‘shacks,’” *Fire Saf. J.*, vol. 91, no. March,  
522 pp. 997–1006, 2017.
- 523 [24] F.P. Incropera and D.P. Dewitt, *Fundamentals of Heat and Mass Transfer*, 5th ed.  
524 John Wiley and Sons, Chichester, 2002.
- 525 [25] Pilkington, “Transmission Properties of Windows July 85 Glaverbel, Reflective  
526 Glazing Monsanto, Solar Control,” *Clim. United Kingdom*.
- 527 [26] “IBM SPSS software.” [Online]. Available: [https://www.ibm.com/analytics/spss-  
528 statistics-software](https://www.ibm.com/analytics/spss-statistics-software). [Accessed: 01-Sep-2019].
- 529
- 530

531

532 **HIGHLIGHTS:**

- 533 • Thermally thin small scale compartment tests conducted with 4 different fuel loads.
- 534 • FDS model validated for small scale under ventilated compartment fire.
- 535 • Numerical parametric study: ventilation effect and wall’s thermal properties.
- 536 • An empirical correlation for  $\dot{Q}_{FO}$  for thermally thin compartments was generated.
- 537 • Sensitivity analysis: main heat transfer parameters for thermally thick/thin walls.

538

539 **LIST OF FIGURES**

540 **Fig. 1.** Quarter scale ISO-9705 compartment (open ceiling for demonstration).....4

541 **Fig. 2.** Measurements’ locations (Not to scale) .....4

542 **Fig. 3.** (a) Cell size ( $\Delta = 10, 5,$  and  $2.5$  cm) sensitivity analysis simulations of test 40\_11 for

543 gas layer temperature at TC\_LF\_5, and (b) for radiative heat flux at 60 cm from the door .....5

544 **Fig. 4.** HRR-time curves evaluation in all tests .....6

545 **Fig. 5.** Gas layer temperatures for all tests at the top of the left front thermocouple tree

546 (TC\_L\_F\_5).....6

547 **Fig. 6.** (a) total and external HRR-time curves for Test 32\_1 and Test 40\_1 (FDS) .....7

548 **Fig. 7.** (a) Comparison between the experimental and numerical gas layer temperature-time

549 curves Test 32\_1 and (b) Comparison between the experimental and numerical gas layer

550 temperature-time curves for Test 40\_1 (Top thermocouples [TC\_5] at two corners).....8

551 **Fig. 8.** Comparison between the experimntal and numerical results for the thermocouples 1→

552 4 of the left front thermocouple tree for Test 40\_1 .....8

553 **Fig. 9.** Comparison between the experimental and numerical velocity-time curves at (a)the

554 top and (b) the middle flow probes locations.....9

555 **Fig. 10.** Comparison between the experimental and numerical Heat Flux-time curves at 60

556 cm and 45 cm from the (a) door and (b) the side wall .....9

557 **Fig.11.** Rate of heat release at the onset of flashover (QFO) as a function of the overall heat

558 transfer coefficient ( $U_{Wall+C}$ ) for several boundary materials and ventilation conditions..... 12

559 **Fig. 12.** Rate of heat release at the onset of flashover (QFO) as a function of the radiative heat

560 transfer coefficient ( $h_{rad}$ ) of the internal walls, for several boundary materials and ventilation

561 conditions..... 13

562 **Fig. 13.** Rate of heat release at the onset of flashover (QFO): comparison of Eq. (5) outputs

563 and results from FDS used as inputs to fit Eq. (5). Blue markers denote data conditions used

564 to fit Eq. (5). Red markers denote external computational validation data used to test the new

565 correlation ..... 13

566